Performance of Hybrid Binary and Non-Binary Turbo Decoding Schemes for LTE and DVB-RCS Standards

Yogesh Beeharry[1†],
Tulsi P. Fowdur[2], and **Krishnaraj M. S. Soyjaudah**[3], Non-members

ABSTRACT

Binary and Non-Binary Turbo codes have been deployed in several digital communication standards to perform error correction. In order to enhance their error performance, several schemes such as Joint Source Channel Decoding (JSCD), extrinsic information scaling mechanisms, and prioritised QAM constellation mapping have been proposed for improving the error performance of error correcting codes. In this paper, hybrid schemes comprising of JSCD, regression based extrinsic information scaling, and prioritised 16-Quadrature Amplitude Modulation (QAM) with binary and non-binary Turbo codes have been presented. Significant improvement in error performance has been observed with the proposed scheme as compared to the conventional one. The hybrid scheme in the case of binary symmetric and asymmetric LTE Turbo codes, and triple binary Turbo codes outperform the conventional scheme by 0.8 dB on average. With duo-binary Turbo codes for the DVB-RCS standard, the hybrid scheme outperforms the conventional one with an average gain of 0.9 dB in BER performance.

Keywords: Binary LTE Turbo codes, Non-Binary Turbo codes, JSCD, Regression based scaling, Prioritised QAM

1. INTRODUCTION

Following the bound established in communication theory by Shannon in 1948 [1], several research works have been carried out with the aim of finding codes which could approach that limit. As such, Berrou and his colleagues came up with Turbo codes [2] in 1993 which significantly closed the gap towards the Shannon limit. Low Density Parity Check (LDPC) code was also re-discovered in 1996 [3] after its development by Gallager in 1963 [4]. Several communication standards have adopted Turbo codes as the error correcting code. For example, mobile telephony standards like 3G and 4G make extensive use of Turbo codes [5, 6]. Joint Source Channel Decoding (JSCD) schemes [7] significantly improve the error performance of communication systems. Furthermore, extrinsic information scaling techniques have shown to enhance the error performance of Turbo codes. Optimised hierarchical Quadrature Amplitude Modulation (QAM) scheme impacts the error performance of Turbo codes positively and recently several works have revealed the advantages that can be derived by incorporating it in the Turbo coding system. An overview is given in the next section.

Recently, the authors of [8] have proposed a technique called the flip and check algorithm which enables the lowering of the error floor of Turbo codes. The proposed method highly depends on the identification of the least reliable bits through the Turbo decoding process. Results have demonstrated that gains of one order of magnitude could be reached in terms of error rate performance. The work presents the hardware implementation of the technique and addresses the feasibility and hardware complexity as well. In [9], the authors have extended the condition for a Quadratic Permutation Polynomial (QPP) to be equivalent to an Almost Regular Permutation (ARP) interleaver, for Cubic Permutation Polynomial (CPP). It has been shown that the CPP interleavers are always equivalent to an ARP interleaver with disorder degree greater than one and smaller than the interleaver length, when the prime factorization of the interleaver length contains at least one prime number to a power higher than one and it fulfils the conditions for which there are true CPPs for the considered length. The work of [10], proposed a new underwater Turbo-code optical communication system with compatibility to partial erasure channel. Results demonstrate that the proposed system outperforms the conventional parallel Turbo-code system without the arrangement of parity bit stream by 1.3 dB at a Bit Error Rate (BER) of 10^{-5}.

In [1], the authors have proposed a joint decoding scheme for polar codes by taking into account information from both the channel and the source. Additionally, a list-size adaptive joint decoding is also implemented which reduces the decoding complexity.

Manuscript received on November 18, 2017 ; revised on September 26, 2018.
The authors are with Department of Electrical and Electronic Engineering, University of Mauritius, Réduit, Mauritius, E-mail : y.beeharry@uom.ac.mu[1], p.fowdur@uom.ac.mu[2], ssoyjaudah@uom.ac.mu[3]
† Corresponding author.

Results demonstrate that the proposed joint decoding schemes outperform stand-alone polar codes by over 0.6 dB. The authors of [2] have considered the problem of joint decoding and data fusion in the context of data gathering by widely deployed sensor networks. An illustration of the performance of the joint decoder for different correlation setups with different number of sensors is provided. Results demonstrate promising enhancements in error performance compared to the conventional decoding where the correlation knowledge is not fully employed in the decoder. The work of [3] proposed a novel decoding method for the Linear Index coding scheme using Joint Source Channel Coding (JSCC) capable of compressing the source data up to its entropy by making use of channel codes. It has been shown that the proposed scheme enhances the bandwidth efficiency of the transmitted data and increases the robustness under channel mismatch conditions as well.

The authors of [4] present a study on the influence of the extrinsic information scaling coefficient (eic) value on the Bit and Frame Error Rate (BER or FER) for the binary and duo-binary Turbo codes. The decoding algorithms used for simulations were Maximum A-posteriori Probability (MAP) and Maximum Logarithmic MAP (Max Log MAP). Results demonstrate that the MAP algorithm performance could be improved using eic <1 to scale the extrinsic information. In [5], a new extrinsic information scaling mechanism for enhancing the error performance of Long Term Evolution (LTE) Turbo codes has been presented. Simulations have been performed using Quadrature Phase Shift Keying (QPSK) modulation and 16-QAM with code-rates $1/3$ and $1/2$. Results demonstrate that a significant improvement in error performance can be obtained compared to the conventional scheme as well as the one employing Sign Difference Ratio (SDR) scaling technique.

In [6]. Lüders *et al.* have applied the technique of prioritisation QAM constellation mapping which is achieved by making use of the Unequal Error Protection (UEP) property of the QAM constellation such that an increased protection is provided to the systematic information bits. The authors of [7] have proposed a system combining prioritised constellation mapping, adaptive Sign Difference Ratio (SDR) based extrinsic information scaling, and Joint Source Channel Decoding (JSCD) in order to enhance the error performance of Turbo coded 64-QAM. The results demonstrate that combining these techniques can help achieve a gain of 2.5 dB on average compared to a conventional Turbo coded 64-QAM system at Bit Error Rates (BERs) above 10^{-1}. As an extended work of [7], the work in [8] studies the error performance of LTE Turbo codes with the same combination of techniques. Additionally, the prioritised constellation mapping is investigated with both 16-QAM and 64-QAM. The results presented demonstrate that with 16-QAM, the combination of all the techniques help achieve an average gain of 1.7 dB over the conventional scheme at BERs above 10^{-1}. With 64-QAM, a performance gain of 3 dB on average is obtained compared to the conventional scheme. Hierarchical Quadrature Amplitude Modulation (HQAM) allows for transmission with uneven level of priority when using constellations with non-uniform spacing. In [9], the authors have proposed an Adaptive HQAM (A-HQAM) mechanism with a regular adjustment of the ratios between the constellation spacing. This modification aims at increasing the transmission efficiency and is based on the channel quality. The simulation results demonstrate that the proposed A-HQAM increases the transmission efficiency, and provides a reduced Peak to Average Power Ratio (PAPR). Additionally, the implementation of a practical A-HQAM is presented allowing the successful demodulation of the received signal with no knowledge of the varying transmission parameters [9]. In [10], an analysis of the performance of 16-QAM was done by applying an information theoretical approach. Based on this approach, a quantitative evaluation is performed to find the amount by which the hierarchical 16-QAM outperforms the conventional non-hierarchical 16-QAM. The results demonstrate that the gain obtained with hierarchical 16-QAM depends on the data rate ratio and the coverage. Finally, the work in [11] proposed the simulation and analysis of HQAM compared to conventional QAM. Different modulation parameters for the HQAM have been used and tested with the transmission of grey images over AWGN wireless channel.

The scheme presented in this work is a hybrid source-channel coding technique using JSCD, regression-based extrinsic information scaling, and prioritised 16-QAM with binary and non-binary Turbo codes. In contrast to schemes using JSCD, extrinsic information scaling, or prioritised QAM independently, the proposed scheme combines all these schemes together in both cases of binary and non-binary Turbo codes. The hybrid system performs prioritisation by placing the systematic information on the most protected points of the constellation, makes use of a-priori source statistics in the first decoder, and scales the extrinsic information throughout the iterative decoding process with the scale factor based on regression analysis. The proposed hybrid schemes provide significant average gains as compared to the ones with conventional decoding only in cases when both binary and non-binary Turbo codes are used independently.

The organization of this paper is as follows. The complete system model is presented in Section 2. The simulation results and analysis are presented in Section 3. Section 4 concludes the paper and proposes some possible future works.

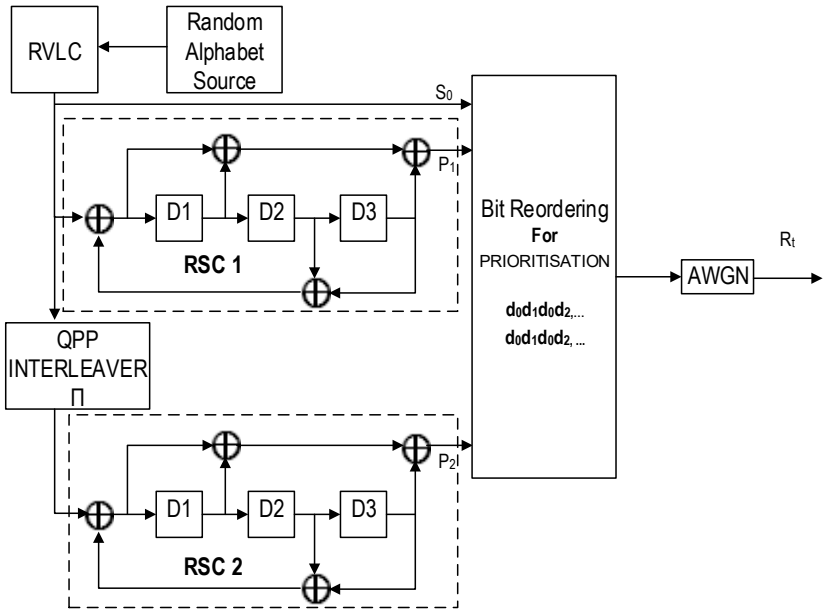

Fig.1: *Complete transmitter system diagram with binary symmetric LTE Turbo codes.*

2. SYSTEM MODEL

This section describes how the hybrid scheme is implemented by incorporating JSCD, regression based extrinsic information scaling, and prioritized 16-QAM together with binary and non-binary Turbo codes.

2.1 Hybrid Binary LTE Turbo Codes

The system's block diagram for the transmitter side of binary symmetric LTE Turbo code is shown in Fig. 1. Symbols generated from the random alphabet source are encoded using a Reversible Variable Length Code (RVLC) encoder. The information bits are sent through the encoder in blocks of length equal to 6144 bits which is the maximum packet length used with LTE Turbo codes. The systematic and parity bits are re-ordered for prioritisation to be performed and give more protection to the systematics information bits. The technique of prioritisation is then used to map groups of four bits to a QAM constellation. The modulated symbols are then transmitted over an AWGN channel.

The symbols used in the Fig. 1 are defined as follows:
S_0: The systematic information bits
P_1: The parity information from the upper Turbo encoder
P_2: The parity information from the lower Turbo encoder
R_t: The received noisy information from the channel

Fig. 2 shows the constellation for Hierarchical modulation with 16-QAM. The constellation with $\alpha = 1.0$ is the conventional one used with LTE Turbo codes [8]. The constellation points in each quadrant

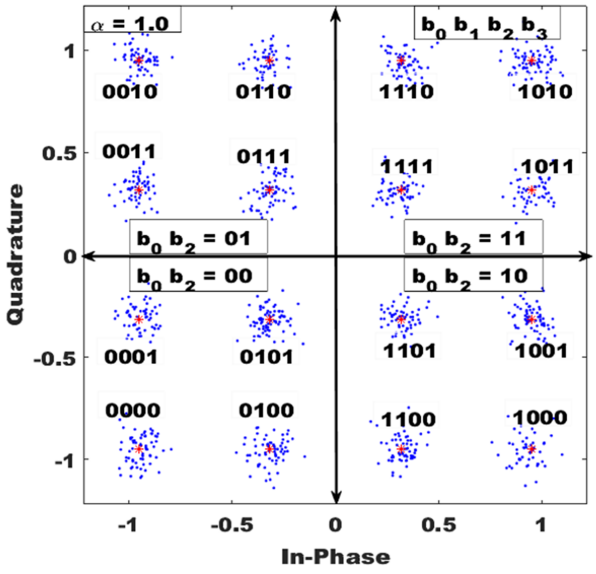

Fig.2: *Constellation for Hierarchical modulation with 16-QAM and* $\alpha = 1.0$.

have the first and third bits in common. These bit positions are used for prioritising the systematics bits. The constellation in Fig. 3 is that of the conventional 16-QAM with $\alpha = 1.0$ and noisy modulated information. The multiplexing is performed in such a way that when prioritisation is employed, the systematic bits are placed at the highest priority positions. The first and third bit positions have highest priority with the 16-QAM constellation used in this work.

At the receiver side, as shown in Fig. 3, the noisy information is demodulated into LLRs corresponding to the transmitted systematic and parity bits. These

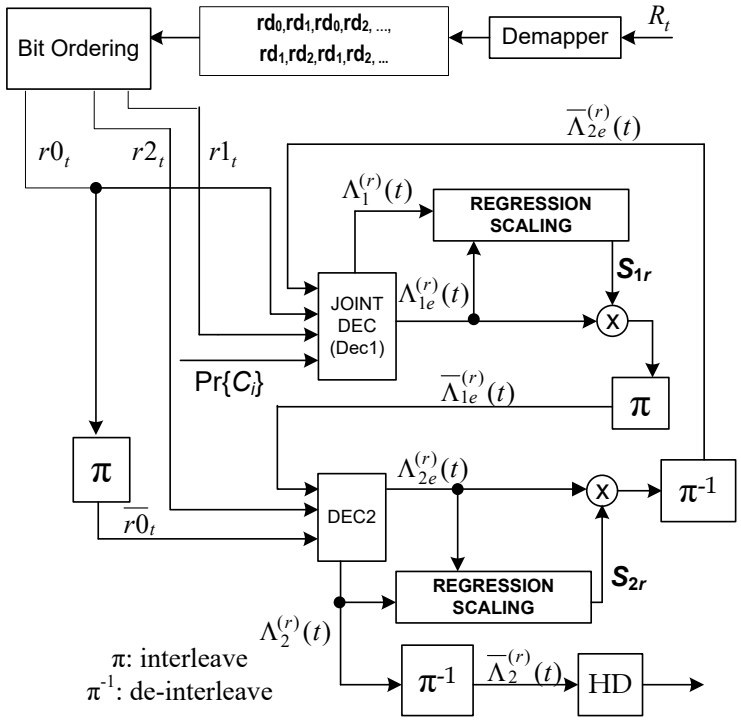

Fig.3: *Complete Receiver System Diagram.*

are then fed to the parallel concatenation of Turbo decoders corresponding to each encoder at the transmitter side. Decoder 1 performs joint decoding by making use of the a-priori source statistics. The a-posteriori and extrinsic LLRs from both decoders are fed to a Regression scaling block which computes the coefficient to be used to scale the extrinsic LLR before being fed back to the other decoder at each half-iteration. When the maximum number of decoding iterations is reached, a hard-decision is performed on the de-interleaved a-posteriori LLRs from Decoder 2 and the estimated bits are finally compared to the transmitted ones for error rate computation.

The symbols used in Fig. 3 are defined as follows:
$r0_t$: received noisy information pertaining to the systematic information from the transmitter
$\overline{r0}_t$: recieved noisy information pertaining to the interleaved systematic information from the transmitter
$r1_t$: received noisy information pertaining to the upper parity information from the transmitter
$r2_t$: received noisy information pertaining to the lower parity information from the transmitter
$Pr\{C_i\}$: A-priori source statistics
$\Lambda_1^{(r)}(t)$: A-posteriori LLR from Decoder 1
$\Lambda_{1e}^{(r)}(t)$: Extrinsic LLR from Decoder 1
$\overline{\Lambda}_{1e}^{(r)}(t)$: Interleaved Extrinsic LLR from Decoder 1
$\Lambda_2^{(r)}(t)$: A-posteriori LLR from Decoder 2
$\overline{\Lambda}_2^{(r)}(t)$: Interleaved A-posteriori LLR from Decoder 2
$\Lambda_{2e}^{(r)}(t)$: Extrinsic LLR from Decoder 2
$\overline{\Lambda}_{2e}^{(r)}(t)$: Interleaved Extrinsic LLR from Decoder 2
S_{1r}: Scale factor for extrinsic LLR from Decoder 1
S_{2r}: Scale factor for extrinsic LLR from Decoder 2

A detailed explanation together with equations for JSCD and regression based extrinsic information scaling with binary LTE Turbo codes are given in [5, 8, 12]. Based on the equations provided independently in the different works, a new equation is presented for the computation of the extrinsic LLR in the first decoder. The composite equation for extrinsic information from the first decoder combined with JSCD and extrinsic information scaling is computed as in Eq. (1).

2.2 Hybrid Non-Binary Turbo Codes

The complete hybrid system for Non-Binary Turbo codes is shown in Fig. 4. The overall process is almost similar to the system for Binary LTE Turbo codes.

The complete encoding system is shown in Fig. 5. The RVLC source [13] is used for the random generation of symbols. All the variable-length packets are combined to form a single bit stream which is then grouped into segments of size 2N or 3N from which couples/triplets of size N are formed.

Circular coding is an adaptation of the tail biting process and ensures that at the end of the encoding operation, the encoder goes back to the initial starting state. This allows for the data decoding to be represented by a circular trellis. The state is known

$$\Lambda_{1e}^{(r)}(t) = (S_{1r})\Bigg\{\Bigg[\max\left(\overline{\alpha}_{t-1}^{1} + \left\{\log\left[Pr_t^1(1)\right] - \left(\frac{\left[r0_t - x0_t\right]^2 + \left[r1_t - x1_t\right]^2}{2\sigma^2}\right) + \log\left[\Pr(C_1)\right]\right\} + \overline{\beta}_t^1(l)\right)$$
$$- \max\left(\overline{\alpha}_{t-1}^{1} + \left\{\log\left[Pr_t^1(0)\right] - \left(\frac{\left[r0_t - x0_t\right]^2 + \left[r1_t - x1_t\right]^2}{2\sigma^2}\right) + \log\left[\Pr(C_0)\right]\right\} + \overline{\beta}_t^1(l)\right)\Bigg]$$
$$- L_c(r0_t) - S_{2r}\left(\overline{\Lambda}_{2e}^{(r)}(t)\right)\Bigg\} \quad (1)$$

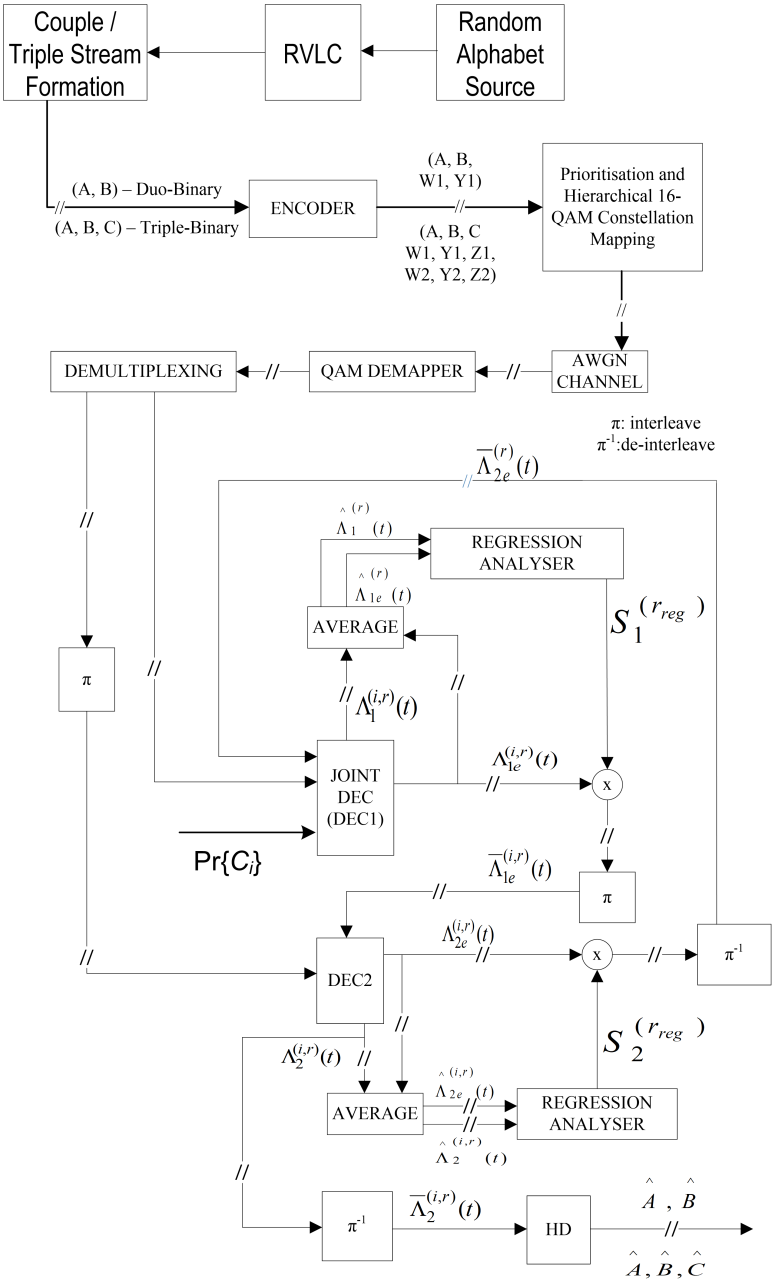

Fig.4: *Complete hybrid system for Non-Binary Turbo Codes.*

as the circular state - S_c. The circular states corresponding to each state and couples/triplets of size N for double binary and triple binary codes are given in [14–16]. After the encoding of the couples/triplets by the non-binary encoder, the output is modulated before transmission. QPSK modulation is used with

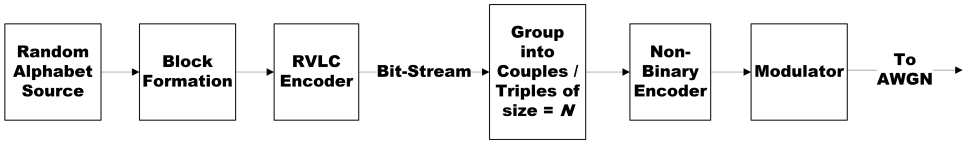

Fig.5: *Complete encoding system.*

duo-binary turbo codes and 8PSK modulation is used with triple binary turbo codes. The complete structures of the encoders and constellation mappings for each modulation scheme are given in [17].

The intermediate states are used to establish distinct decoding paths for each symbol. The transition probability from state $S_{t-1} = M$ to $S_t = M'$, where M, $M' \in$ {F, IA, IB, IC, ID, IE and IF} given an input bit $C_t = i$ at time t, is given as follows [18]:

$$\Pr(S_t = M', C_t = i | S_{t-1} = M) = \frac{\sum_{i \in f(S_t)} P(i)}{\sum_{i \in f(S_{t-1})} P(i)} \quad (2)$$

where, $f(S_t)$ is the set of symbols connected to the state S_t and $f(S_{t-1})$ is the set of symbols connected to the state S_{t-1}. For example, consider that $S_{t-1} =$ F and for a given input bit $C_t = 1$ $S_t =$ IB. Thus, $f(S_t) = \{C\}$ and $f(S_{t-1}) =$ {A1, B1, C1, D1 and E1}.

$$\Pr(S_t = \text{IB}, C_t = 1 | S_{t-1} = \text{F}) = \frac{P_{C1}}{P_{A1} + P_{B1} + P_{C1} + P_{D1} + P_{E1}} = P_{C1} = P201 \quad (3)$$

P201, in this case, represents the transition from state 2 to state 0 with an input bit 1 on the bit-level trellis. As explained in [18], the symbol a-priori probabilities for the non-binary schemes are extracted using a time stretched VLC trellis. For duo binary the time-stretched trellis is as shown in Fig. 6. Consider for example the starting state F at t0 with an input bit $C_t = 0$ reaches state IA at time t1 and from state IA with input bit $C_t = 0$ state F is reached at time t2. Hence, an input symbol (00) from state F at time t0 reaches state F at time t2. Similarly, all the possible inputs and transitions can be obtained from the time-stretched trellis.

The state transition probabilities are derived by considering all the transitions in both the bit-level and symbol level-trellis [18].

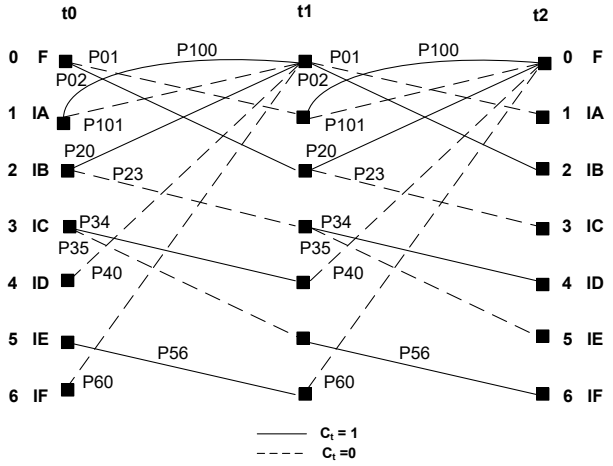

Fig.6: *Time-stretched bit-level trellis for duo binary turbo codes.*

$$\Pr(S_{t+1} = \text{F}, C_t = 00 | S_{t-1} = \text{F}) = \Big[\Pr(S_t = \text{IA}, C_t = 0 | S_{t-1} = \text{F}) * \Pr(S_{t+1} = \text{F}, C_t = 0 | S_t = \text{IA})\Big] = (PA + PB) * \frac{PA}{(PA + PB)} = P010 * P100 \quad (4)$$

The same approach is used with triple binary. The time-stretched trellis used extends from t0 to t3. Consider the starting state to be F at time instant t0 which reaches state IA at time t1 with input bit $C_t = 0$. From the state IA, with input bit $C_t = 0$, state F is reached at time t2 and finally state IA is reached at time t3 with a third input bit $C_t = 0$. Therefore with an input symbol (000) at time t0 from initial state F, state IA is reached at time t3. The general equation to obtain the symbol a-priori probabilities is [18]:

$$\Pr(S_{t+k-1}, C | S_{t-1}) = \prod_{n=1}^{k} \Pr(S_{t+n-1}, C_{t+n-1} | S_{t+n-2}) = \Pr\{C_i\} \quad (5)$$

where, $\Pr\{C_i\}$ is used to denote the a-priori probability of symbol C_i.

When $k = 1$, the bit a-priori probabilities are obtained. The symbol a-priori probabilities for duo binary and triple binary are obtained with $k = 2$ and

$k = 3$ respectively. The complete block diagram of the decoding system is as shown in Fig. 2. The iterative turbo decoding consists of two component decoders connected via an interleaver which is similar to the one used on the encoding side. Circular codes are very well suited to the turbo decoding concept since for these codes, the decoding of a received sequence consists of going round a circular trellis. In order to reduce the computational complexity, the suboptimum Max-Log MAP decoding algorithm is used for the non-binary CRSC codes with JSCD. With the conventional symbol-level decoding mechanism, duobinary Turbo codes are used with Q-PSK modulation and triple-binary Turbo codes are used with 8-PSK modulation. In order to achieve higher spectral efficiency with non-binary Turbo codes using 16-QAM or higher order modulations, symbol-level decoding with bit-level LLRs is needed [19, 20]. The equations with both decoding techniques are described in the following sub-sections.

2.2.1 JSCD with Conventional Symbol-Level Decoding

The method in [18] is used to modify the Max-Log MAP algorithm and incorporate the symbol a-priori probabilities in the joint decoder. The joint decoder is obtained by combining the symbol level trellis with the channel decoder trellis which leads to a modified branch metric. Let the branch transition probability at time t from state $S_{t-1} = l'$ to $S_t = l$ associated with input symbol $C_t = U$, (where U can take values 0, 1, 2 and 3 for duo binary and 0, 1, 2, 3, 4, 5, 6 and 7 for triple binary) [17] be denoted by $\overline{\gamma}_t^{1,U} s\,(l', l)$. Also, let $r0$, $r1$ and $r2$ be the received noisy vectors of the systematic and parity information. The modified branch metric (that takes into account the symbol a-priori probabilities) for the joint decoder is given as:

$$\overline{\gamma}_t^{1,U} s(l', l) = p\left(u_t^2 = U\right) - \left(\left[r0_t^I - x0_t^{I(U)}(l)\right]^2 + \left[r0_t^Q - x0_t^{Q(U)}(l)\right]^2 + \left[r1_t^I - x1_t^{I(U)}(l)\right]^2 + \left[r1_t^Q - x1_t^{Q(U)}(l)\right]^2 \right) + \log\left(\Pr\{C_i\}\right) \quad (6)$$

where, $p\left(u_t^2 = U\right)$ is the a-priori symbol probability of symbol i obtained from the second decoder. $x0_t^{I(U)}(l)$ and $x0_t^{Q(U)}(l)$ are the modulated in-phase and quadrature components of the complex systematic symbol $x0$ at time t which is associated with the transition $S_{t-1} = l'$ to $S_t = l$ and input symbol i. $x1_t^{I(U)}(l)$ and $x1_t^{Q(U)}(l)$ represent the same for symbol $x1$. $r0_t^I$ and $r0_t^Q$ are the in-phase and quadrature components of $r0$, while $r1_t^I$ and $r1_t^Q$ are the in-phase and quadrature components of $r1$. $\Pr\{C_i\}$ is the symbol a-priori probability. The forward and backward recursive variables are computed as the following for the first decoder:

$$\overline{\alpha}_t^1 = log \sum_{l'=0}^{M_J^1-1} e^{\overline{\alpha}_{t-1}^1 + \overline{\gamma}_t^{1,i} s(l',l)} \quad (7)$$

Using the Max-log-map simplification, Eq. (6) can be expressed as follows:

$$\overline{\alpha}_t^1\,(l) = \max\left(\overline{\alpha}_{t-1}^1 + \overline{\gamma}_t^{1,i} s\,(l', l)\right), \text{ for } 0 \le l' \le M_J^1 - 1 \quad (8)$$

$$\overline{\beta}_t^1 = log \sum_{l'=0}^{M_J^1-1} e^{\overline{\alpha}_{t+1}^1 + \overline{\gamma}_{t+1}^{1,i} s(l',l)} \quad (9)$$

Using the Max-log-map simplification, Eq. (8) can be expressed as follows:

$$\overline{\beta}_t^1(l) = \max\left(\overline{\beta}_{t+1}^1 + \overline{\gamma}_{t+1}^{1,i} s\,(l', l)\right), \text{ for } 0 \le l' \le M_J^1 - 1 \quad (10)$$

$$\Lambda_{1,U}(t) = log\left[\frac{\sum_{l'=0}^{M_J^1-1} e^{\overline{\alpha}_{t-1}^1 + \overline{\gamma}_t^{1,U} s\left(l',l\right) + \overline{\beta}_t^1(l)}}{\sum_{l'=0}^{M_J^1-1} e^{\overline{\alpha}_{t-1}^1 + \overline{\gamma}_t^{1,0} s\left(l',l\right) + \overline{\beta}_t^1(l)}}\right] \quad (11)$$

Using the Max-log-map simplification, Eq. (10) can be expressed as follows:

$$\Lambda_{1,U}(t) = \max\left(\overline{\alpha}_{t-1}^1 + \overline{\gamma}_t^{1,U} s\,(l', l) + \overline{\beta}_t^1\,(l)\right) - \max\left(\overline{\alpha}_{t-1}^1 + \overline{\gamma}_t^{1,0} s\,(l', l) + \overline{\beta}_t^1\,(l)\right), \text{ for } 0 \le l' \le M_J^1 - 1 \quad (12)$$

where, $\overline{\alpha}_t^1$ is the forward recursive variable of decoder 1, $\overline{\beta}_t^1$ is the backward recursive variable of decoder 1, M_J^1 is the number of states in the first decoder and $\Lambda_{1,U}(t)$ is the log-likelihood ratio (LLR) of symbol U where, $U \in \{1,\ 2 \text{ and } 3\}$ for duo binary turbo codes and $U \in \{1,\ 2,\ 3,\ 4,\ 5,\ 6 \text{ and } 7\}$ for triple binary turbo codes [17].

The extrinsic LLR from decoder 1 with extrinsic information scaling and a-priori LLRs incorporated with source statistics for JSCD is expressed as:

$$\Lambda_{1e,U}^{(r)}(t) = (S_{1r})\Big[\Lambda_{1,U}(t) - L_c(r0_t) - S_{2r}\left(\overline{\Lambda}_{2e,U}^{(r)}(t)\right)\Big] \quad (13)$$

The equations for decoder 2 are now presented. The branch metric of the second decoder in conventional decoding is given as:

$$\overline{\gamma}_t^{2,U} = p(u_t^1 = U) - \Bigg(\left[\overline{r0}_t^I - x0_t^{I(U)}(l)\right]^2 + \left[\overline{r0}_t^Q - x0_t^{Q(U)}(l)\right]^2 + \left[r2_t^I - x2_t^{I(U)}(l)\right]^2 + \left[r2_t^Q - x2_t^{Q(U)}(l)\right]^2 \Bigg) \quad (14)$$

where, $p(u_t^1 = U)$ is the a-priori symbol probability of symbol i obtained from the first decoder. $x0_t^{I(U)}(l)$ and $x0_t^{Q(U)}(l)$ are the modulated in-phase and quadrature components of the complex systematic symbol $x0$ at time t which is associated with the transition $S_{t-1} = l'$ to $S_t = l$ and input symbol U. $x2_t^{I(U)}(l)$ and $x2_t^{Q(U)}(l)$ represent the same for symbol $x2$. $\overline{r0}_t^I$ and $\overline{r0}_t^Q$ are the in-phase and quadrature components of the interleaved version of $r0$, while $r2_t^I$ and $r2_t^Q$ are the in-phase and quadrature components of $r2$. The forward and backward recursive variables are computed as the following:

$$\overline{\alpha}_t^2 = log \sum_{l'=0}^{M_S^2-1} e^{\overline{\alpha}_{t-1}^2 + \overline{\gamma}_t^{2,U}(l',l)} \quad (15)$$

Using the Max-log-map simplification, Eq. (13) can be expressed as follows:

$$\overline{\alpha}_t^2(l) = \max\left(\overline{\alpha}_{t-1}^2 + \overline{\gamma}_t^{2,U}(l',l)\right), \text{ for } 0 \le l' \le M_S^2 - 1 \quad (16)$$

$$\overline{\beta}_t^2 = log \sum_{l'=0}^{M_S^2-1} e^{\overline{\alpha}_{t+1}^2 + \overline{\gamma}_{t+1}^{2,U}(l',l)} \quad (17)$$

Using the Max-log-map simplification, Eq. (15) can be expressed as follows:

$$\overline{\beta}_t^2(l) = \max\left(\overline{\beta}_{t+1}^2 + \overline{\gamma}_{t+1}^{2,U}(l',l)\right), \text{for } 0 \le l' \le M_S^2 - 1 \quad (18)$$

$$\Lambda_{2,U}(t) = log\left[\frac{\sum_{l'=0}^{M_S^2-1} e^{\overline{\alpha}_{t-1}^2 + \overline{\gamma}_t^{2,U}(l',l) + \overline{\beta}_t^2(l)}}{\sum_{l'=0}^{M_S^2-1} e^{\overline{\alpha}_{t-1}^2 + \overline{\gamma}_t^{2,0}(l',l) + \overline{\beta}_t^2(l)}}\right] \quad (19)$$

Using the Max-log-map simplification, Eq. (17) can be expressed as follows:

$$\Lambda_{2,U}(t) = \max\left(\overline{\alpha}_{t-1}^2 + \overline{\gamma_t^{2,U}}(l',l) + \overline{\beta}_t^2(l)\right) - \max\left(\overline{\alpha}_{t-1}^2 + \overline{\gamma}_t^{2,0}(l',l) + \overline{\beta}_t^2(l)\right), \text{ for } 0 \le l' \le M_S^2 - 1 \quad (20)$$

where, M_S^2 denotes the number of states in the second decoder. The equations for the extrinsic information output from both decoders for double binary are explained in [21]. The extrinsic information scaling for non-binary Turbo codes has been incorporated by computing the regression correlation coefficient between the means of the different symbol-level a-posteriori and extrinsic LLRs.

The extrinsic LLR from decoder 2 with extrinsic information scaling and conventional a-priori LLRs is expressed as:

$$\Lambda_{2e,U}^{(r)}(t) = (S_{2r})\Big[\Lambda_{2,U}(t) - L_c(\overline{r0}_t) - S_{1r}\left(\overline{\Lambda}_{1e,U}^{(r)}(t)\right)\Big] \quad (21)$$

The number of states, M_J^1, in the joint decoder (for both non binary schemes being analysed) is greater than the number of states in the second decoder, M_S^2 due to the incorporation of the states of the symbol level trellis of the VLC decoder. The addition of the a-priori source information is only possible for the first decoder, since the interleaver breaks the one-to-one correspondence between the VLC tree and the decoding trellis in the second decoder [22]. The second decoder, therefore, operates normally with the parameters of Eq. (14)–21.

2.2.2 JSCD with Symbol-Level Decoding using Bit-Level LLRs

The symbol-level decoding using bit-level LLRs is described in [19, 20]. In view to achieve high spectral efficiency with non-binary Turbo codes using high order modulation schemes such as 16-QAM, this technique is used. The decoding equations in the JSCD context used in this case are presented next.

The modified branch metric (that takes into account the symbol a-priori probabilities) for the joint decoder with duo-binary Turbo codes is given as:

$$\overline{\gamma}_t^{1,U}(l',l) = \left(S_2^{(r_{reg})}\right)\left(\overline{\Lambda}_{2,e}^U(t)\right) + \frac{L_c}{2}\Bigg([(rA_t)\cdot(xA_t)] + [(rB_t)\cdot(xB_t)] + [(rY_{1t})\cdot(xY_{1t})] + [(rW_{1t})\cdot(xW_{1t})] \Bigg) + \log\left(\Pr\{C_i\}\right) \quad (22)$$

The equations for the forward and backward recursive variables, and the a-posteriori LLRs are similar to those for the conventional mechanism. A similar approach is used with triple-binary Turbo codes.

3. SIMULATION RESULTS

The results obtained with binary symmetric, binary asymmetric, duo-binary, and triple-binary Turbo codes are presented in this section.

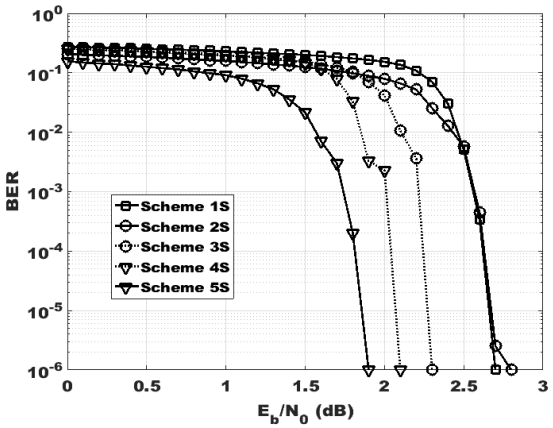

Fig.7: *BER performance for Binary symmetric LTE Turbo codes with $N = 6144$, 16-QAM, code-rate = 1/3.*

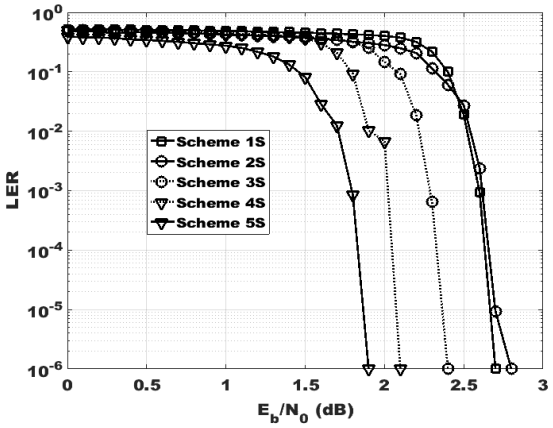

Fig.8: *LER performance for Binary symmetric LTE Turbo codes with $N = 6144$, 16-QAM, code-rate = 1/3.*

3.1 Results with Binary Symmetric LTE Turbo codes

The performances of the following schemes for Binary symmetric LTE Turbo codes have been evaluated through simulation.

1. Scheme 1S: Conventional decoding with binary symmetric LTE Turbo codes.
2. Scheme 2S: Binary symmetric LTE Turbo codes with prioritised QAM constellation mapping only.
3. Scheme 3S: Binary symmetric LTE Turbo codes with Regression based extrinsic information scaling only.
4. Scheme 4S: Binary symmetric LTE Turbo codes with JSCD only.
5. Scheme 5S: Binary symmetric LTE Turbo codes with JSCD, Regression based extrinsic information scaling, and prioritised QAM constellation mapping with equidistant constellation points.

The detailed simulation parameters are as follows: the generator polynomial in octal for both upper and lower encoders of the LTE Turbo code is given as G = [1, g1/g2], where g1 = 15 and g2 = 13; Packet-length, $N = 6144$; Code-rate = 1/3; Maximum number of iterations: 12; Modulations: 16-QAM; Channel: complex AWGN

The graphs of Bit Error Rate (BER) and Levenshtein Error Rate (LER) as a function of E_b/N_0 have been plotted over the E_b/N_0 range: 0 dB $\leq E_b/N_0 \leq$ 3 dB in steps of 0.1 dB for 16-QAM. Fig. 7 shows the graph of BER against E_b/N_0 for symmetric LTE Turbo codes. It can be observed from the graph that Scheme 5S outperforms the conventional Scheme 1S by 0.8 dB on average. A similar trend of average gain of 0.8 dB in terms of LER performance is observed in Fig. 8. The trade-off for this gain in performance is the increased complexity with the usage of source statistics in the case of JSCD and computation of the regression based scale factor.

3.2 Results with Binary Asymmetric LTE Turbo codes

The BER performances of the following schemes for binary asymmetric LTE Turbo codes have been evaluated through simulation:

1. Scheme 1A: Conventional decoding with binary asymmetric LTE Turbo codes.
2. Scheme 2A: Binary asymmetric LTE Turbo codes with prioritised QAM constellation mapping only.
3. Scheme 3A: Binary asymmetric LTE Turbo codes with Regression based extrinsic information scaling only.
4. Scheme 4A: Binary asymmetric LTE Turbo codes with JSCD only.
5. Scheme 5A: Binary asymmetric LTE Turbo codes with JSCD, Regression based extrinsic information scaling, and prioritised QAM constellation mapping with equidistant constellation points.

In this case, the generator polynomial for the upper encoder remains the same as for symmetric LTE Turbo codes. The generator polynomial in octal for the lower encoder of the LTE Turbo code is given as G = [1, g1/g2], where g1 = 13 and g2 = 15.

The graphs of Bit Error Rate (BER) and Levenshtein Error Rate (LER) as a function of E_b/N_0 have been plotted over the E_b/N_0 range: 0 dB $\leq E_b/N_0 \leq$ 3 dB in steps of 0.1 dB for 16-QAM. Fig. 9 shows the graph of BER against E_b/N_0 for asymmetric LTE Turbo codes. It can be observed from the graph that both Scheme 5A outperforms the conventional Scheme 1A by 0.8 dB on average. A similar trend of average gain of 0.8 dB in terms of LER performance is observed in Fig. 10. The gain in performance is obtained at the expense of increased complexity with the usage of source statistics in the case of JSCD and the computation of the regression based scale factor.

The BER and LER graphs of the binary symmetric and asymmetric LTE Turbo codes reveal that

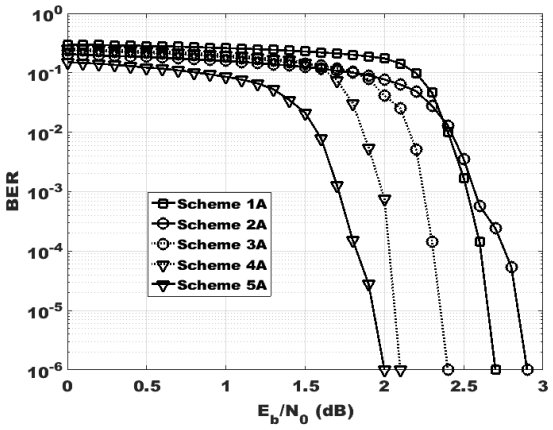

Fig.9: *BER performance for Binary asymmetric LTE Turbo codes.*

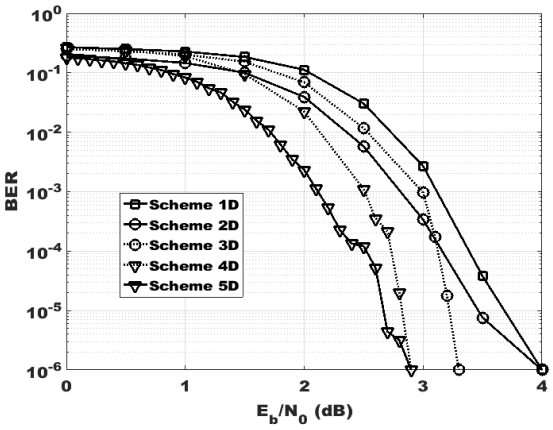

Fig.11: *BER performance for duo-binary Turbo codes.*

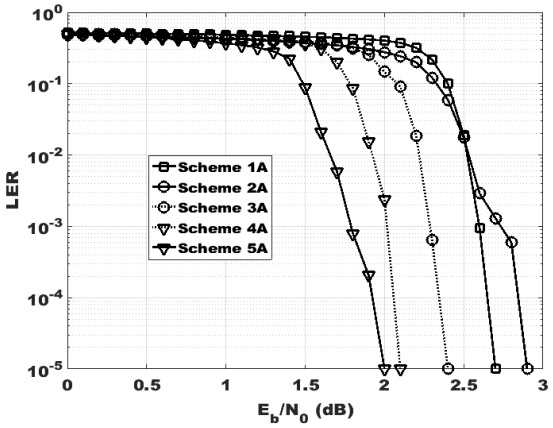

Fig.10: *LER performance for Binary asymmetric LTE Turbo codes.*

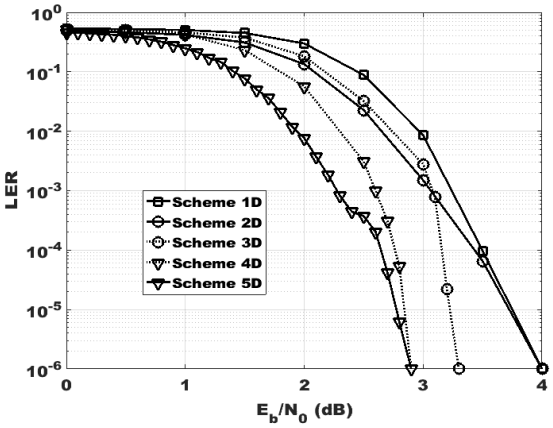

Fig.12: *LER performance for duo-binary Turbo codes.*

with packet lengths of 6144, 16-QAM and code-rate of 1/3, the hybrid Scheme 5S demonstrates better performance compared to Scheme 5A. Additionally, all the other schemes with symmetric LTE Turbo codes demonstrate better performance (Fig. 7 and Fig. 8) compared to their counterparts with asymmetric LTE Turbo codes (Fig. 9 and Fig. 10). Asymmetric LTE Turbo codes perform better than symmetric LTE Turbo codes for medium packet lengths as per the literature [23].

3.3 Results with Duo-Binary Turbo codes

The BER performances of the following schemes for duo-binary Turbo codes have been evaluated through simulation:
1. Scheme 1D: Conventional decoding with duo-binary Turbo codes.
2. Scheme 2D: Duo-Binary Turbo codes with prioritised QAM constellation mapping only.
3. Scheme 3D: Duo-Binary Turbo codes with Regression based extrinsic information scaling only.
4. Scheme 4D: Duo-Binary Turbo codes with JSCD only.
5. Scheme 5D: Duo-Binary Turbo codes with JSCD, Regression based extrinsic information scaling, and prioritised QAM constellation mapping with equidistant constellation points.

The graphs of Bit Error Rate (BER) and Levenshtein Error Rate (LER) as a function of E_b/N_0 have been plotted over the E_b/N_0 range: 0 dB $\leq E_b/N_0 \leq$ 4 dB in steps of 0.1 dB for 16-QAM. Fig. 11 shows the graph of BER against E_b/N_0 for duo-bianry Turbo codes. It can be observed from the graph that Scheme 5D outperforms the conventional Scheme 1D by 0.9 dB on average. A similar trend of average gain of 0.6 dB in terms of LER performance is observed in Fig. 12. The trade-off for this gain in performance is the increased complexity with the usage of source statistics in the case of JSCD and computation of the regression based scale factor.

3.4 Results with Triple-Binary Turbo codes

The BER performances of the following schemes for triple-binary LTE Turbo codes have been evalu-

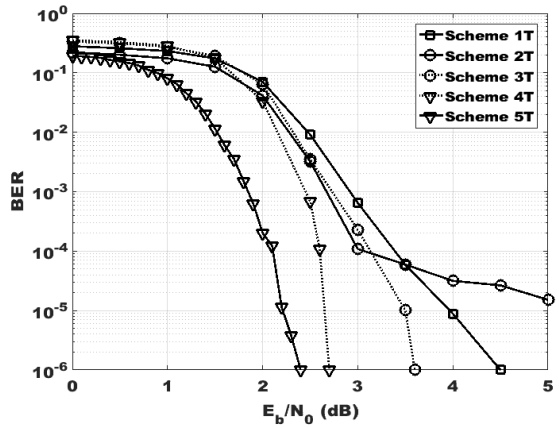

Fig.13: *BER performance for triple-binary Turbo codes.*

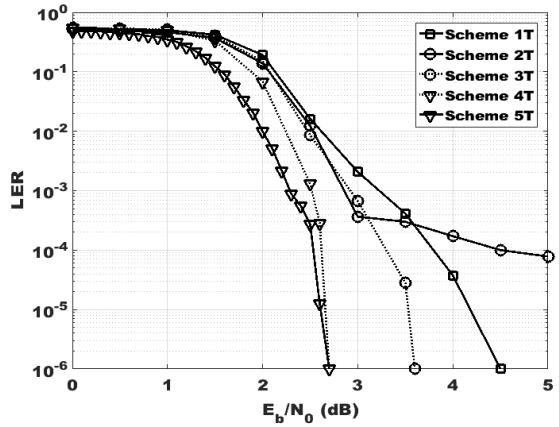

Fig.14: *LER performance for triple-binary Turbo codes.*

ated through simulation:
1. Scheme 1T: Conventional decoding with triple-binary Turbo codes.
2. Scheme 2T: Triple-Binary Turbo codes with prioritised QAM constellation mapping only.
3. Scheme 3T: Triple-Binary Turbo codes with Regression based extrinsic information scaling only.
4. Scheme 4T: Triple-Binary Turbo codes with JSCD only.
5. Scheme 5T: Triple-Binary Turbo codes with JSCD, Regression based extrinsic information scaling, and prioritised QAM constellation mapping with equidistant constellation points.

The graphs of Bit Error Rate (BER) and Levenshtein Error Rate (LER) as a function of E_b/N_0 have been plotted over the E_b/N_0 range: 0 dB $\leq E_b/N_0 \leq$ 4.5 dB in steps of 0.1 dB for 16-QAM modulation. Fig. 13 shows the graph of BER against E_b/N_0 for triple-binary Turbo codes. It can be observed from the graph that Scheme 5T outperforms the conventional Scheme 1T by 0.8 dB on average. A similar trend in terms of LER performance is observed in Fig. 14. The trade-off for this gain in performance is the increased complexity with the usage of source statistics in the case of JSCD and computation of the regression based scale factor.

Scheme 2T in the above case has a deviated performance as compared to the other schemes. This is an anomalous behaviour with Scheme 2T below BER 10^{-3}, whereby it starts exhibiting an error-floor earlier than the conventional Scheme 1T.

4. CONCLUSION

In this paper, a hybrid scheme comprising of JSCD, regression based extrinsic information scaling, and prioritised 16-QAM binary and non-binary Turbo codes have been presented.

The different schemes have also been simulated separately to demonstrate the trend towards improved performance. Prioritisation deals with the placement of the systematic information bits on the most protected positions on the QAM constellation. The technique for extrinsic information scaling computes a scale factor based on regression analysis using the a-posteriori and extrinsic LLRs output from each decoder at each half iteration. Extrinsic information scaling technique provides further gain in performance as compared to prioritisation. Furthermore, the JSCD scheme which uses a-priori source statistics in decoder 1 provides more gain in error performance in contrast to the former two techniques. The last scheme combines all the three schemes together to form the hybrid system, which provides a combined gain in error performance as compared to the separately used mechanisms.

Significant improvement in error performance has been observed with the proposed scheme as compared to the conventional one.

The hybrid scheme in the case of binary symmetric LTE Turbo codes outperform the conventional scheme by 0.8 dB on average. The same trend in error performance gain is obtained in the case of binary asymmetric LTE Turbo codes. With duo-binary Turbo codes, the hybrid scheme outperforms the conventional one with an average gain of 0.9 dB in BER performance. In the case of triple binary Turbo codes, the hybrid scheme provides an average gain of 0.8 dB in error performance over the conventional scheme.

Several interesting future works can be proposed from the work in this paper. One straightforward extension would be to perform the analysis with different packet lengths, code-rates, and modulation schemes. A more challenging future work would be to come up with mathematical modifications which would further increase the error performance of the hybrid scheme with optimized parameters for hierarchical modulation compared to that without optimized parameters for hierarchical modulation in both the waterfall and error-floor regions. Furthermore, machine learning prediction models can be formu-

lated to accurately set optimized parameters for hierarchical modulation depending on the parameters used at the transmitter side and channel quality estimate.

ACKNOWLEDGEMENT

The authors would like to thank the University of Mauritius for providing the necessary facilities for conducting this research and the Tertiary Education Commission for its financial support.

References

[1] Y. Wang, M. Qin, K. R. Narayanan, A. Jiang and Z. Bandic, "Joint Source-Channel Decoding of Polar Codes for Language-Based Sources," in *IEEE Global Communications Conference (GLOBECOM)*, 2016.

[2] A. Zribi, T. Matsumoto and R. Pyndiah, "Joint source-channe decoding for LDPC-coded error-corrupted binary Markov sources," in *International Conference on Computing, Networking and Communications (ICNC)*, 2016.

[3] R. Mahmood, Q. Huang and W. Zulin, "A novel decoding method for Linear Index Joint Source-Channel Coding schemes," in *13th International Bhurban Conference on Applied Sciences and Technology (IBCAST)*, 2016.

[4] H. Balta and C. Douillard, "On the influence of the extrinsic information scaling coefficient on the performance of single and double binary turbo codes," *AECE - Advances in Electrical and Computer Engineering Journal*, vol. 2013, no. 2, pp. 77–84, 2013.

[5] T. P. Fowdur, Y. Beeharry and K. M. S. Soyjaudah, "A Novel scaling and Stopping Mechanism for LTE Turbo Codes based on Regression Analysis," *Annals of Telecommunications*, vol. 71, no. 7, pp. 369–388, 2016.

[6] H. Lüders, A. Minwegen and P. Vary, "Improving UMTS LTE Performance by UEP in High Order Modulation," in *7th International Workshop on Multi-Carrier Systems & Systems (MC-SS 2009)*, Herrsching, Germany, 2009.

[7] T. P. Fowdur, Y. Beeharry and K. M. S. Soyjaudah, "Performance of Turbo Coded 64-QAM with Joint Source Channel Decoding, Adaptive Scaling and Prioritised Constellation Mapping," in *CTRQ, 6th International Conference on Communication Theory, Reliability, and Quality of Service*, Venice, Italy, April, 2013.

[8] T. P. Fowdur, Y. Beeharry and K. M. S. Soyjaudah, "Performance of LTE Turbo Codes with Joint Source Channel Decoding, Adaptive Scaling and Prioritised QAM Constellation Mapping," *International Journal on Advances in Telecommunications*, vol. 6, no. 3 & 4, pp. 143–152, 2013.

[9] H. Mukhtar and M. El-Tarhuni, "An Adaptive Hierarchical QAM Scheme for Enhanced Bandwidth and Power Utilization," *IEEE Transactions on Communications*, vol. 60, no. 8, pp. 2275–2284, August, 2012.

[10] J. Lee, K. A. Kim, J. S. Jung and S. C. Lee, "Analytical Performance Evaluatioin of Hierarchical 16-QAM for Multicast/Broadcast Transmission," *IEEE Communications Letters*, vol. 16, no. 10, pp. 1536–1539, August, 2012.

[11] M. A. Kader, F. Ghani and R. Badlishah, "Development and Performance Evaluation of Hierarchical Quadrature Amplitude Modulation (HQAM) for Image transmission over Wireless Channels," in *3rd International Conference on Computation Intelligence, Modelling &Simulation*, Langkawi, September, 2011.

[12] Y. Beeharry, T. P. Fowdur and K. M. S. Soyjaudah, "Performance Analysis of Symmetric and Assymetric LTE Turbo codes with Prioritisation and Regression based Scaling," in *1st International Conference on Electrical, Electronic and Communications Engineering (ELECOM)*, Bagatelle, Mauritius, 2016.

[13] Y. Takishima, M. Wada and H. Murakami, "Reversible Variable Length Codes," *IEEE Trans. Commun.*, vol. 43, pp. 158–162, 1995.

[14] C. Douillard, C. Berou and M. Jezequel, "Multiple parallel concatenation (CRSC) codes," *Annals of Telecommunications*, vol. 64, no. 3–4, pp. 166–172, 1999.

[15] Y. Gao and M. R. Soleymani, "Triple binary circular recursive systematic convolutional turbo codes," in *5th International Symposium on Wireless Personal Multimedia Communications*, 2002.

[16] M. R. Soleymani and Y. Gao, "Spectrally efficient non-binary turbo codes: Beyond DVB-RCS standard," in *Proceedings of 21st Biennial Symposium on Communications*, vol. 3, pp. 951–955, 2002.

[17] T. P. Fowdur and Y. Beni, "Reliable JPEG image transmission using unequal error protection with modified non-binary turbo codes," *IARIA*, vol. 5, no. 3–4, pp. 284–296, 2012.

[18] T. P. Fowdur and K. M. S. Soyjaudah, "Performance of Joint source-channel decoding with iterative bit combining and detection," *Annals of Telecommunications*, vol. 63, no. 7–8, pp. 409–423, August 2008.

[19] H. Balta, M. Kovaci, C. Botiz and C. Poenaru, "Bit Decoding versus Symbol Decoding in Multi-Binary Turbo Decoders," in *4th International Conference of Engineering Technologies, ICET 2009*, Novi, Sad, 2009.

[20] Y. Beeharry, T. P. Fowdur and K. M. S. Sojaudah, "Symbol-Level Decoding Algorithms for Duo-Binary Turbo Codes," *IIUM Journal*, vol.

18, no. 1, 2017.

[21] Y. O. C. Mouhamedou, 2005. [Online]. Available: http://www-mmsp.ece.mcgill.ca/MMSP/Theses/2005/Ould-Cheikh-MouhamedouT2005.pdf. [Accessed December 2012].

[22] M. Jeanne, J. Carlach and P. Siohan, "Joint Source-Channel decoding of variable-length codes for convolutional codes and turbo codes," *IEEE Transactions on Communications*, vol. 53, no. 1, pp. 10–15, 2005.

[23] M. Suryanegara, M. Khalimudin and N. Raharya, "The comparison between Asymmetric Turbo Code using O' QPP Interleaver and LTE Turbo Code," in *International Conference on Quality in Research (QiR)*, Lombok, Indonesia, 2015.

Yogesh Beeharry holds a BEng (Hons) Electronics and Communications engineering with First class honours from the University of Mauritius. He was also the recipient of the Mrs. L. F. Lim Fat Engineering Gold medal, the British American Tobacco Undergraduate Scholarship Scheme and the MPhil/PhD scholarship from the Tertiary Education Commission of Mauritius. He is presently Lecturer and a PhD student in the field of Telecommunications Engineering at the University of Mauritius. His main research interests are: error control coding, Turbo codes, source and channel coding, Big Data real-time analytics, Internet of Things, and Machine Learning.

Tulsi P. Fowdur received his BEng (Hons) degree in Electronic and Communication Engineering with first class honours from the University of Mauritius in 2004. He was also the recipient of a Gold medal for having produced the best degree project at the Faculty of Engineering in 2004. In 2005 he obtained a full-time PhD scholarship from the Tertiary Education Commission of Mauritius and was awarded his PhD degree in Electrical and Electronic Engineering in 2010 by the University of Mauritius. He is presently Associate Professor at the Department of Electrical and Electronic Engineering at the University of Mauritius. His research interests include Coding Theory, Multimedia and Wireless Communications, Networking and Security.

Krishnaraj M. S. Soyjaudah had a long and successful career at the University of Mauritius where he contributed significantly in academic research, namely in the fields of Communications Engineering and Computer Science and Engineering. He has about 220 research publications. He successfully supervised to completion two post-doctoral research fellows and 16 PhDs. His expertise in research is also regularly solicited by overseas universities for the examination of PhD theses. He was the recipient of the UK Commonwealth Scholarship on two occasions, namely to read for a BSc(Hons) in Physics at Queen Mary College and fora MSc in Digital Electronics at Kings College, University of London. He holds a PhD in Digital Communication Engineering. He further read for a LLB (Hons) from London University and a PGD in legal studies at the bar from Manchester law school. He is a Barrister Member of the Middle Temple, London, UK. He was the Chairman of Mauritius Qualifications Authority from 2002 to 2005. He was a Board Director of Multicarrier (Mauritius) Ltd from 2001 to May 2016 and a Board Member and Technical Expert in the Energy Efficient Management Office. Professor Soyjaudah was the Executive Director of the ICTA. He was also the Executive Director of the Tertiary Education Commission. Professor Soyjaudah is also a Senior Member of the Institute of Electrical and Electronics Engineers.